IMPEDANCE-BASED FEEDBACK CONTROL OF COMBINATORIAL DROPLET
INJECTIONS ON A VALVE-ACTUATED MICROFLUIDIC DEVICE

by
Brant Axt

A thesis submitted to Johns Hopkins University in conformity with the requirements
for the degree of Master of Science in Biomedical Engineering

Baltimore, Maryland
May, 2017

ABSTRACT

Droplet microfluidics has found use in many biological assay applications as a means of high-throughput sample processing. One of the challenges of the technology, however, is the ability to control and merge droplets on-demand as they flow through the microdevices. It is in the interest of developing lab-on-chip devices to be able to program additive mixing steps for more complex multistep and multiplex assays. Existing technologies to merge droplets are either passive in nature or rely on open-loop control systems, making them vulnerable to errors during high throughput or long duration experimentation. Herein is described and demonstrated a microfluidic valve-based device for the purpose of combinatorial droplet injection at any stage in a multistep assay. Microfluidic valves are used to control fluid flow, generate droplets, and inject droplets on-demand, while on-chip impedance measurements taken in real time are used as feedback to accurately time the droplet injections. The presented system is compared to open-loop control and its reliability is demonstrated over long time durations. Additionally, the system is shown to be able to differentiate between phosphate-buffered saline and deionized water droplets, and programmatically inject an arbitrary pattern based on droplet content on-demand.

THESIS COMMITTEE:

Tza-Huei Wang
Professor
Mechanical Engineering & Biomedical Engineering Depts.
Sidney Kimmel Comprehensive Cancer Center
Institute for NanoBioTechnology
Johns Hopkins University

Eileen Haase
Senior Lecturer
Interim Director, Undergraduate Program
Program Chair Applied Biomedical Engineering
Johns Hopkins University

Andreas Andreou
Professor of Electrical and Computer Engineering
Johns Hopkins University

PREFACE / ACKNLOWLEDGEMENTS

TABLE OF CONTENTS

LIST OF FIGURES

1 BACKGROUND

1.1 Brief History of Microfluidic Devices

The study of microfluidics at its most fundamental is a study of fluid dynamics on the scale of micrometers. At this size, conventional fluid forces like fluid inertia and the effects of gravity become relatively small compared to forces such as fluid viscosity and surface tension. As a result, Reynolds number at this scale are very small, leading to an environment dominated by laminar flow.

A microfluidic device is an apparatus designed with constricting geometries for working with and analyzing fluids at the micrometer scale. The first microfluidic devices by this definition were glass capillaries used by Poiseuille to study fluid dynamics as early as the 1830s[1], but the first microfluidic system by modern standards wasn't created until the late 1970s, when a gas chromatographer was fabricated in a wafer of silicon[2]. Throughout the 1980s, not much focus was given to microfluidic development until a seminal paper by Manz et al. in 1990 summarized the benefits that these "miniaturized total analysis systems" (µTAS) could have on chemical analysis, such as more efficient gas chromatography, faster electrophoresis, and the capability for simultaneous measurements in multiple channels.[3] As a result, microfluidic platforms began to see more use in these respective areas[4]. Capillary electrophoresis in particular drew a lot of attention as it had clearly benefitted from the higher sensitivities and resolutions possible only with microfluidic flow.[5] Also during this time, researchers began investigating the use of microfluidics in blood rheology since the dimension were at the same scale as the system in vivo[6,7]. However, despite the new interest, microfluidics failed to see widespread use as the

device fabrication process was time consuming and required advanced machinery. This was because microfluidic devices were a technology transfer from the success of the miniaturization of microelectronics. As a result, the devices were made from the same materials, namely silicon, glass, and metals, which required extensive labs to work with at the microscale.[2,4,6–10]

Through the 1990s, various research groups began investigating alternative microfluidic materials that could be casted or molded onto a master template, such as plastics and polymers. This would allow microfluidic devices to be more rapidly fabricated and eliminate the issue of single time use. Polydimethylsiloxane (PMDS), which would eventually become the front runner for microfluidic devices, was first used in their manufacturing towards the end of the 1990s.[11,12] As PDMS became more popular, research groups were able to fabricate devices outside of clean rooms by ordering a master mold in silicon from a supplier and creating hundreds of copies of the device by spin coating PDMS on top of the template in a process called soft lithography. In addition to the time and cost savings, PDMS also had other physical properties that benefitted study of biological material. Its surface chemistry could be controlled via well-known techniques[13], its permeability to gases like carbon dioxide and oxygen enabled cell culturing on-chip[14], and its flexibility facilitated the creation of extremely useful features like monolithic fluid control valves.[15] With decreased cost for fabrication and increased accessibility, the number of microfluidics papers being published rose quickly after the turn of the millennium.

However, despite improvements in materials and accessibility, scaling remained a problem for microfluidic device application in industry. Many industrial

applications required very high-throughput processing, but device size linearly increased with the number of parallel experiments to be run on the same chip because parallel analysis required parallel channels. To remedy this, researchers began to investigate droplet based devices in the early 2000s in order to achieve parallelization of experiments within single channels.[16]

1.2 Basic Principles of Droplet Microfluidics Systems

When two immiscible fluids are mixed together, it is possible to create droplet suspensions of one fluid within the other. Each of these droplets can act as an individual reaction chamber as it travels through the device.[17] As mentioned previously, this gives the benefit of carrying out parallel reactions without the need for parallel fluid channels, conserving device size and increasing throughput.[18] When compared to conventional minute parallel reaction chambers such as microtiter plates, droplet microfluidics drastically reduces material needs and cost while also preventing of issues of sample loss from pipetting or non-specific adsorption. [19–21] As a result of these benefits, droplet microfluidics devices have found application in many areas of study, such as single molecule analysis[22], cell sorting[23], disease detection[24], and enzyme kinematics[25].

For some assays, it is enough to simply generate and then detect the droplets, but many other assays require additional complexity. A complete droplet microfluidics system might need to be capable of droplet creation, processing, reagent addition, and droplet detection. There are a plethora of approaches to accomplish each of these steps and each has benefits and drawbacks depending upon

the unique needs of the envisioned application. Some of the basic technologies are described below.

Droplet Creation

The first design choice of any droplet-based microfluidic system is the method used to generate droplets. This selection depends on the prioritized drop characteristics for the system. The following section will summarize a few of the most common methods of droplet generation and their benefits and shortcomings.

Perhaps the simplest forms of droplet generation are passive systems like cross-flow[16,26], co-flow[27], or flow-focusing systems[28]. The size distribution and generation frequency of these droplets are dependent on the relative flow rates, as well as the densities and viscosities of the two fluid phases. Droplets are created in the dispersed phase through instabilities caused by shear forces, which balance the viscous and inertial forces of the fluid against the interfacial forces.[29] The resultant droplets are highly monodisperse and suitable for high frequency droplet generation. However, while the fluid velocities and pressures can be adjusted to control the size of the droplets, these modalities lack the ability for droplet creation on demand and are difficult to implement in systems where the droplets requires indexing or individual labeling.

Active droplet generation in contrast introduces much more control over droplet generation but requires introducing external energy sources. Some methods of active control only allow for controlled tuning of the droplet size and frequency of generation while others facilitate actual on-demand generation. Methodologies

which create on-demand droplets include direct current (DC) pulses[30,31], laser-induced cavitation[32], and fluid channel deformation by piezoelectric or mechanical valves[33–36]. The laser-induced cavitation has the largest throughput potential with droplet generation recorded at 10 kHz, but the cavitation could be damaging to samples and the optics necessary to operate the microfluidic device would be large and expensive. DC current pulses also add electric charge to the droplets which could interfere with assays through electrolysis. While the microfluidic valves typically result in lower throughput, they are highly programmable and do not affect the properties of the fluids in any way.

Reagent Addition

In most droplet microfluidic devices, reagents are added to the droplets during droplet formation[37], but there many combinatorial or additive assays which require reagent addition at a later time point. Broadly, reagent addition techniques can be split into two categories: droplet coalescence and injection. Coalescence is the merging of individual droplets in proximity to each other, whereas injection involves adding fluid to a droplet from bulk solution.

Droplet coalescence has been achieved with device channel geometry[38,39], electrostatic charge[40], electrocoalescence[41], surface acoustic wave merging[42], pneumatic actuators [43], and magnetic fields [44]. However, despite the diversity of energy sources, the approach to create coalescence is almost always the same. The droplets to be merged are generated in sequence, and the first droplet is slowed or temporarily trapped somewhere in the device, allowing the following droplet to catch

up and join it before carrying forward. One exception is the electrostatic charge method in which the droplets are attracted to each by opposing charges. The main benefits of coalescence over injection is a low chance of cross contamination and the ability for the droplets to be smaller than the channel width. However, the major downside when compared to injection is that more than one additive step is quite complicated to perform and it is very difficult to customize the amount of reagent for each droplet.

Injection of droplets has been achieved with simple cross-flow junctions[45–47], electrowetting injectors[48], and microfluidic valves[49,50]. T-junctions are the simplest to construct, but they are dependent on carefully balanced pressure conditions and are passive in nature, preventing programmability. Electrowetting injectors alter the surface tension of droplets, which are normally very stable, so that when the droplets come in contact with another fluid the fluids join and mix.[48] The downside of this system is that it is likely susceptible to cross contamination and it is difficult to customize the amount of fluid injected on-demand. Microfluidic valves have the added benefit of being able to inject each droplet with a programmable amount of fluid depending on the duration that the valve is open.

Droplet Sensing

No microfluidic total analysis system is complete without a detection point. In droplet-based microfluidics, this means measuring some property of the droplet stream, whether it is just counting the droplets, or measuring the physical properties like volume or content. Modalities for droplet sensing include optical-based detection

such as vision systems[51] and fluorescence spectroscopy[52], or electrode based detection such as amperometry[53], capacitive sensing[54,55], and impedance measurements[56].

Vision systems use algorithms such as edge detection to identify and track droplets as they travel through a device. This is useful for tracking multiple droplets simultaneously but loses applicability because of its requirement for a high speed camera and calibrated optics. Fluorescence detection is a more common optical method, but it often requires that fluorescent tags be added to the samples, which could affect the processing or measurement, and the optical systems aren't easily scalable. Electronic measurements such as capacitance and impedance are label-free and are easily scalable in device design, however it can be very difficult to detect small molecular contents.

1.3 Needs in Automation and Feedback Control

The benefits of droplet-based microfluidics, such as decreased reagent consumption, won't be fully realized until it is successfully implemented in industry on large scale batch processing. However, to replace existing batch processing technologies in industry, microfluidic devices need to match them in terms of automation and versatility. In the agricultural industry, for example, there exists a need for large scale genotyping for crop selection. The current state-of-the-art technology for high throughput processing is Array Tape™ technology (Douglas Scientific).[57] In order to compete with this technology, it will be beneficial for

microfluidics to have feedback control automating various device operations so that long-term, high-throughput sample analysis can be successfully executed.

Feedback control will additionally facilitate more complex device assays. Using the principles described above, droplet based systems have been implemented separately in multistep assays and combinatorial assays, but never in a system capable of both multiple additive steps, and programmable combinatorial mixing. On demand combinatorial droplets have been demonstrated using on-chip and off-chip microfluidic valves[49,50], but without an efficient feedback network the droplets must be merged during droplet generation which limits these combinatorial assays to single step complexity. There is one group that has demonstrated a feedback control system for droplet injecting using fluorescence to locate droplets and programmatically merge reagents using picoinjectors.[48] However, the need for a complex optical detection system mounted on an inverted microscope, in addition to the droplet requiring fluorescent molecules to enable detection, reduces the applicability and scalability of the system. Electrochemical methods of measurement are an attractive alternative for droplet tracking as electrodes are easy to fabricate using the same microfabrication techniques used in soft lithography, they can be more easily scaled and more rapidly prototyped as needed.

In this regard, a system is presented which is capable of tracking droplets in a multiphasic environment for the purpose of successful on-demand addition of reagents to these isolated sub-microliter droplets with great precision. This system implements microfluidic valves for both droplet generation and droplet mixing, with clear potential for scaling.

2 FEEDBACK CONTROL SYSTEM DESIGN

A flowchart of the architecture of the entire feedback control system is shown in Figure 1. The system consists of four main components: A microfluidic device that handles the fluids, a pressure controller that manipulates the microfluidic valves, an impedance spectroscope that measures the impedance of the on-chip electrodes, and a processor that connects the loop by reading the impedance valves and simultaneously directing the pressure controller. Each system component is described in more detail below.
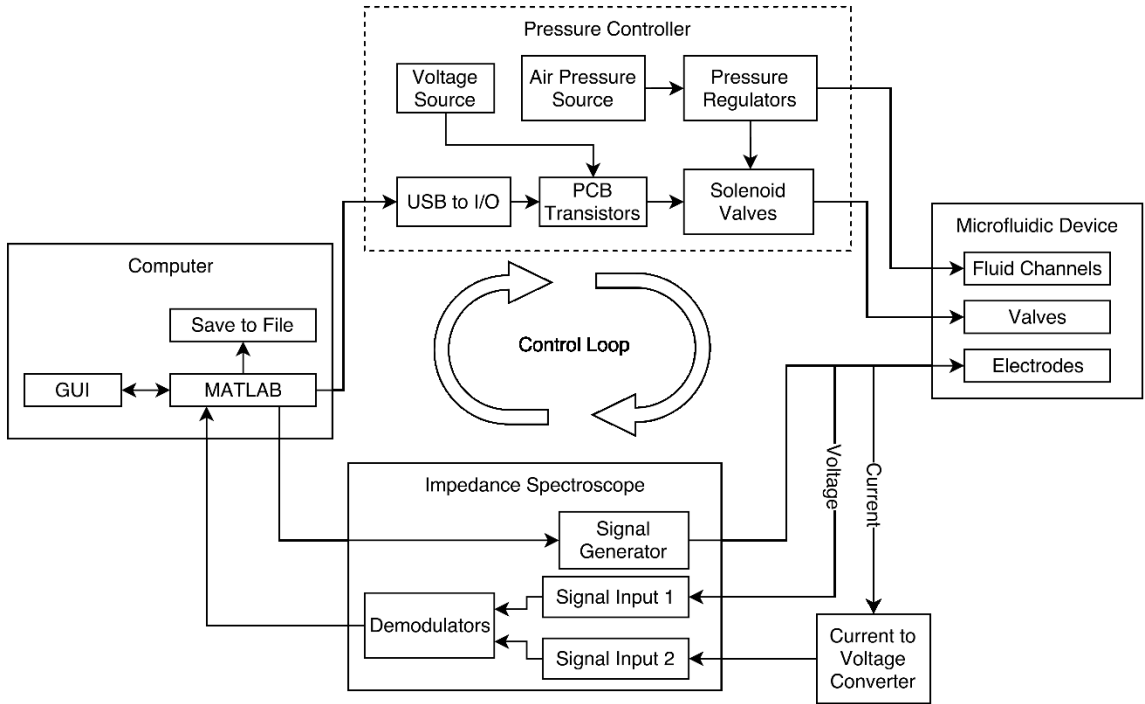
Figure 1: Architecture of the impedance-based feedback control system for the valve-based droplet microfluidic device. MATLAB software on a computer manipulates a pressure controller through a serial communication interface. The pressure controller changes the states of the valves on the device in order to generate and inject droplets. The microfluidic chip controls and processes the droplets. Finally, the feedback loop is completed by the impedance spectroscope that measures the electrode impedance and stores the values for access by MATLAB.

2.1 Microfluidic Device Operation

The microfluidic device used in this study and its operations are presented in Figure 2, which has an annotated photograph of the prototype device with inset illustrations to detail the functional areas. Figure 2a illustrates the droplet generating region of the microdevice, which is capable of generating droplets from any combination of three fluid inlets, each moderated by microfluidic valves. On either side of these fluid inputs are two relief valves (not shown) which open during droplet creation in order to eliminate a pressure drop across the fluid inlets. This is necessary to maintain accurate droplet volumes because the downstream pressure of the main fluid channel changes depending on the amount of droplets in the device. Figure 2b depicts the travel region of the device, which simulates a long processing step that the droplet could undergo in a given assay. For example, it could be necessary to perform a series of heating steps in order to perform PCR within the droplet. The travel region also doubles its functionality as a fluid buffer to dampen the effects of rapidly changing pressures during droplet creation or injection. Figure 2c is a schematic of the injection region of the microdevice where traveling droplets are merged with additional reagents. In this presented device there are three inlets for up to three reagents, but the design could be easily expanded to meet analysis needs. Just upstream of these reagent inlets is a pair of coplanar electrodes that transversely cross the fluid channel. The impedance signal (its phase component shown in Figure 2c) that is measured across these electrodes is analyzed to detect the presence of a droplet. This information is used to accurately time the actuation the microfluidic valves so that successful addition of reagent occurs.
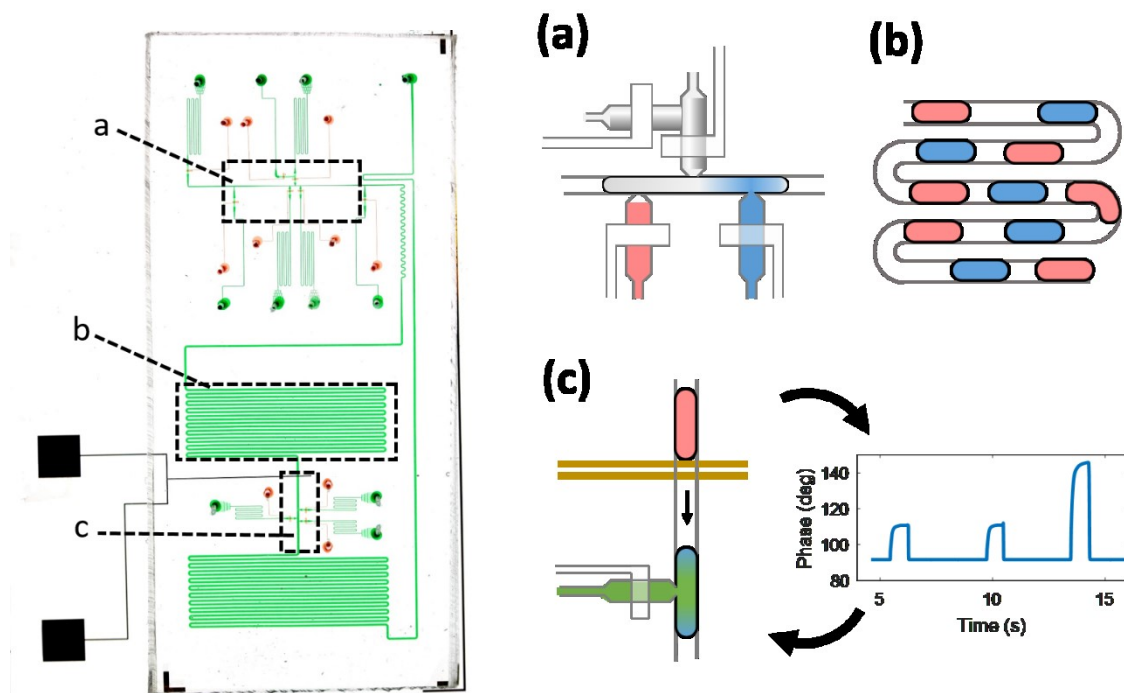
Figure 2: Overview of the microdevice (left) An image of the device with the fluid channels dyed green, the valve control channels dyed orange, and where the electrodes appear as solid black. (a) the droplet generation region, with three potential inlets for samples to be made into droplets. The top inlet has a rinsing channel so different samples can be more quickly loaded; (b) the travel region, to simulate a long processing step that could occur; (c) the injection region, where droplet mixing occurs. A sample phase component of the impedance signal is shown. This signal is used to locate droplets and time injections

2.2   Microfluidic Device Fabrication

The fabrication of the device in this study involves the creation of three functional layers: the substrate with electrodes, the PDMS fluid layer, and the PDMS valve control layer. The fabrication steps involved in assembling this device are illustrated in Figure 3, with further details of the fabrication steps described below.

Electrode Deposition

The electrodes are patterned on top of a 75mm by 50mm by 1mm glass slide (#2947-75X50, Corning) using election-beam deposition and liftoff techniques. In brief, the glass slides are cleaned in acetone, followed by a rinse in isopropanol, and subsequent exposure to oxygen plasma for 3 minutes at 100 watts. Positive photoresist (Microposit® S1813, Microchem Inc.) is spun onto the cleaned glass slides at 2000rpm for 30 seconds, soft baked at 115°C for 90 seconds, and exposed to UV light at 150 mJ/cm^2 intensity for 30 seconds during contact photolithography. The electrode pattern is revealed when the glass slide is then bathed in a developer (Microposit® MF® CD-26, Microchem Inc.). Afterwards, using the e-beam evaporator, a 50nm layer of chrome is deposited on top of the photoresist, followed by a 500nm layer of gold. The underlying photoresist is then dissolved in a lift-off process by submerging the slide in a bath of acetone for 3 hours. This leaves the finished substrate layer with the patterned electrodes.

Template Microfabrication

The master molds for the fluid layer and the valve control layer are fabricated on four inch silicon wafers. For the fluid layer, two steps of photolithography are required to make the rectangular fluid channels and the rounded collapsible valve channels. This process was detailed previously by Quake Labs[15], but briefly, positive photoresist (Microposit® SPR-220, Microchem Inc.) is spun on the wafer at a thickness of 20μm, patterned into valve channels 100μm wide, and hard baked. Then a negative photoresist (Microposit® SU-8 2030, Microchem Inc.) is spun to a thickness of 20μm, patterned for the remaining channels, and hard baked. During the development process, the positive photoresist leaves behind rounded channels that facilitate collapse whereas the negative photoresist results in rectangular channel geometry. The width of the channels range from 50μm in the droplet creation region to 200μm in the travel region. The narrower channel in the droplet creation region serves to elongate the droplets to facilitate combinatorial droplet mixing. With regards to the valve control layer, a single layer of negative photoresist (Microposit® SU-8 2030, Microchem Inc.) is spun on at a thickness of 20μm and patterned into the control channels. The channels above the valves are 100μm wide so that the collapsible intersections are 100μm by 100μm.

Soft Lithography

PDMS is layered onto the previously manufactured master molds through spin coating. For the valve control layer, the PDMS and curing agent are mixed in a 6:1 ratio to promote stiffness and spun onto the mold at 100rpm for 2 minutes followed

by a 5 minute bake at 80°C. In parallel, the PMDS for the fluid layer is mixed in a 15:1 ratio for greater flexibility and spun on at 1300rpm for 1 minute followed by a 4 minute bake at 80°C. This results in a thin membrane on top of the fluid layer template which is able to collapse during pressurization of the valve control layer.

Chip Assembly

For the first stage of assembly, the valve control layer is peeled off its respective template and aligned on to the fluid layer (Figure 3). The two layers of PDMS are allowed to bond permanently by baking for 7 hours at 80°C. An additional layer of 10:1 PDMS (not shown in Figure 3 for simplicity) is poured on top of the bonded layers to increase the PDMS thickness in order to better support the fluid connectors when cured. The layered PDMS assembly is then peeled from the fluid template and access ports are created for the valves and channels by punching through the PDMS with a needle. The layered PDMS assembly is then exposed to oxygen-plasma (60 seconds at 30W) and bonded to the substrate layer patterned with the electrodes. The complete assembly is then baked for a minimum of 5 hours at 80°C to ensure a robust bonding.

Hydrophobic Coating

Prior to experimentation, the PDMS and glass surfaces are made to be hydrophobic through application of a commercial hydrophobic coating agent (Rain-X® Original, ITW Global Brands). First, the assembled microdevice is exposed to oxygen plasma at 30W for 45 seconds. Then the fluid channels are perfused with the

coating and allowed to set for 5 minutes before being flushed with air at 3psi and dried. Rain-X® consists of PDMS suspended in a bath of ethanol with a mix of sulfuric acid to create hydroxyl groups which help it attach to the glass. The resulting coating is essentially a thin coat of PDMS
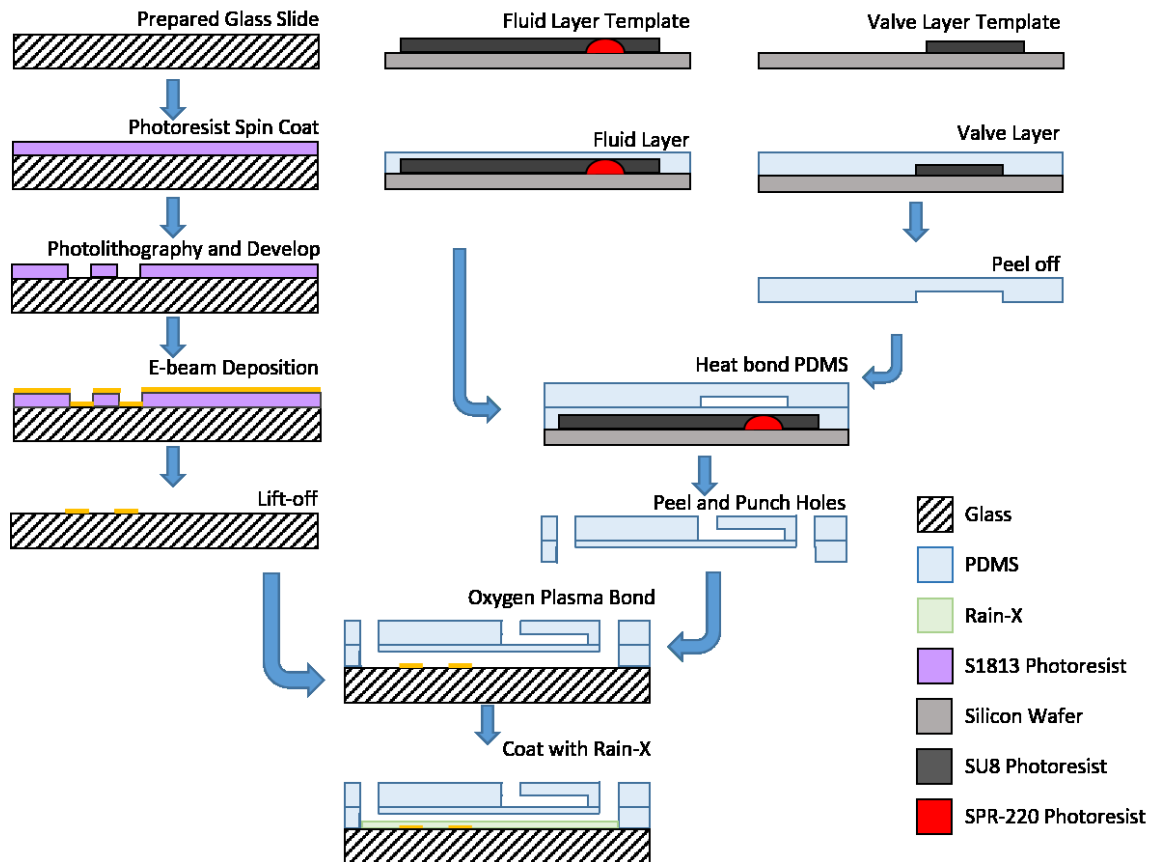
Figure 3: A flow chart of the fabrication and assembly process of the microdevice. On the left is the fabrication process for the substrate and electrodes while on the right are the paths for the two PDMS layers. Not shown are the fabrication steps for the creation of the master molds. The final three layers are assembled using a combination of heat bonding and oxygen plasma bonding before the device is coated with a hydrophobic coating.

2.3   Impedance Measurement System

The electrodes patterned on the glass substrate of the microdevice were designed to behave as a coplanar capacitor which is dependent on the dielectric properties of the surrounding material. In reality, the only insulation in between the electrodes and the main fluid channel is the hydrophobic coating material, which isn't a perfect insulator. Therefore, the electrodes don't behave entirely as a capacitor but rather some equivalent combination of capacitors and resistors in series and parallel. Regardless, the impedance characteristics of the two electrodes depends on the content of the fluid channel. In order to measure the impedance between these electrodes, a four terminal measurement system is implemented, wherein the current through the electrodes and voltage drop across them are measured independently to increase measurement accuracy. The entire circuit for measurement is illustrated in Figure 4. Coaxial cables (50 Ω) are used to connect the various components of the circuit. In order to connect the probes of the coaxial cable to the microfluidic device, bare copper wires are attached to the electrode pads using electrically conductive epoxy (8331S, MG Chemicals). A high-impedance differential amplifier within the spectroscope is used to measure the voltage across the electrodes without drawing current, while a trans-impedance amplifier (HF2TA, Zurich Instruments) converts the current through the electrodes into a voltage signal for sampling. A set of commercial dual-phase demodulators (HF2IS, Zurich Instruments) read the voltage signals and store the real and imaginary components into memory to be accessed at any time by a connected computer via USB interface.

Figure 4: The circuit architecture for the impedance measurement circuit. The impedance spectroscope (HF2IS, Zurich Instruments) generates a signal internally from a numerical oscillator which is transformed into an analog signal by an digital-to-analog converter (DAC) In a four terminal configuration, the voltage drop across the electrodes in the microfluidic device is measured through a high impedance differential amplifier internal to the impedance spectroscope. This signal is converted with an analog-to-digital converter (ADC) before being passed into a dual phase demodulator which outputs values proportional to the real and imaginary components of the signal. This value is stored in a register of a 32-bit processor in order to be accessed by the computer at a later time. The current through the electrodes is converted to a voltage signal by an I/V converter which is essentially a transimpedance amplifier. Then it is similarly passed through an ADC before being split into signal components by a dual phase modular. Internally, the dual phase modulators consist of signal multipliers followed by low pass filters to get voltage signals proportional to the real and imaginary components of the sine waves.

2.4   Microfluidic Valve Control

The microfluidic valves used in our device are commonly known as "Quake Valves" as their design was established previously by the Quake Labs.[15] These valves are pressure actuated, and therefore require a control system to allow on-demand actuation. The control system implemented in our experiments is described in detail by the Quake Laboratories on their website.[58] Briefly, each individual microfluidic valve is connected to a solenoid valve through a length of Tygon® microbore tubing (Cole-Palmer). Each solenoid valve receives pressurized air from a pressure source that is moderated by a pressure control valve. The architecture of the system can be seen in Figure 1 but is elaborated on in more detail in Figure 5. The current to the

solenoid valve is turned on and off by a high-voltage transistor which is connected at the base to a digital input-output controller (Elexol USBIO24 R). The controller is connected to the computer via USB cable in order to communicate with the programmed software.

Figure 5: Valve Controller Block Diagram. (a) The computer with loaded MATLAB software sends commands through the USB to (b) the input-output module for digital signals (Elexol USBIO 24 R). This integrated module sets pin voltages which are connected to the base connection of (d) the transistors. The transistors allow current from (c) the DC voltage source (normally wall outlet with an AC to DC converter) to (g) the solenoid valve. The pressure for the device is supplied by a (f) pressure source which is regulated by a (e) pressure regulator. This pressure line is connected to the (i) microfluidic device through a (h) capillary line which is represented in this block diagram as a constricted orifice.

2.5   Software and Threshold Detection Overview

The software used to automate the microfluidic system was written in MATLAB. Its purpose is to complete the feedback loop by controlling the state of microfluidic valves on the device and periodically sampling the impedance measurements of the electrodes. Additional functionality of the software includes manual control of the valves and also the ability to upload a list of sequential valve commands to be executed in order. A graphical user interface (GUI) was created to allow the user to program the feedback control system while observing the impedance measurements in real time. Its layout is shown below in Figure 6.
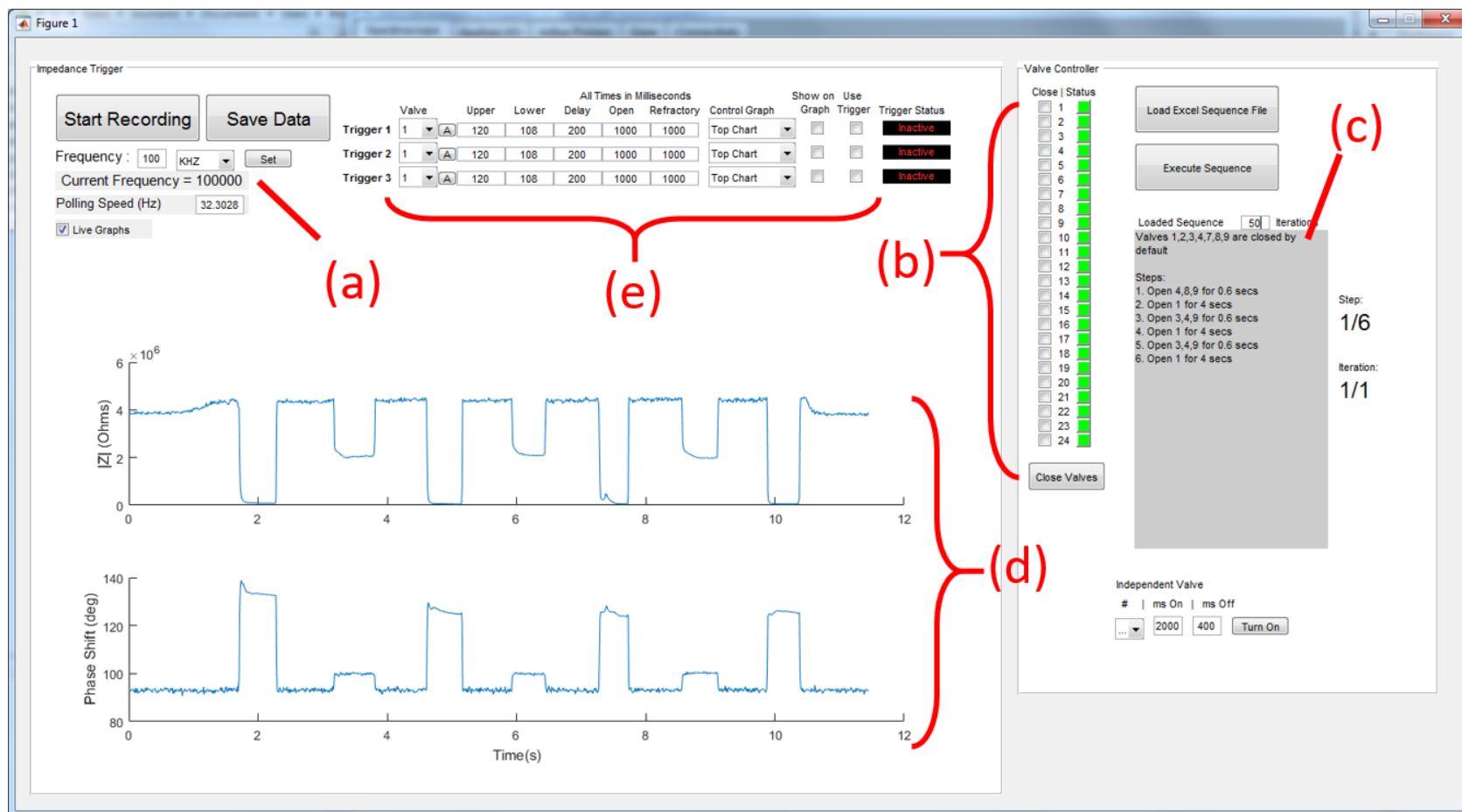
Figure 6: The GUI that the user sees when running experiments with the feedback control system. The various functionalities include (a) setting the operating frequency of the impedance spectroscope, (b) manually operating the microfluidic valves, (c) loading and executing a valve sequence written in an external excel file. (d) Viewing the impedance measurements in real time, and (e) setting the parameters of the injection event. In (e) it is possible to set the boundaries of the threshold, select the graph to base the threshold on, and set the time parameters like delay time, open time, and refractory time..

Using the GUI, the user has the ability to set the parameters of the threshold detection and subsequent injection. The steps from detection of a droplet to successful injection are illustrated below in Figure 7. There are seven unique parameters that the user has control over to tune the system to optimal working conditions. The first parameter is the valve number for the reagent that the user desires to inject into the traveling droplets. Next is the selection of either the phase or the magnitude of impedance for use in creating a threshold. Two more parameters used for the upper and lower bounds of the threshold. Once the droplet crosses the electrode as shown in Figure 7a, the impedance signal will move within the threshold boundaries as in Figure 7e. Once the signal is within the threshold boundaries, a droplet detection event occurs. This begins the timing sequence that consists of three programmable time periods: the delay period, the open period, and the refractory period. First, the delay period is the amount of time it takes for the droplet to travel from the electrodes to the reagent input channel, as shown in Figure 7b. This timer is dependent on the droplet flow rate and the distance between the electrode and the reagent channel. When the delay period timer is finished, the open period timer begins. This is the amount of time that the reagent valve opens for an injection, as shown in Figure 7c. The user sets this duration based on the amount of injection desired. The final timer is for the refractory period, which occurs after injection is finished, and takes place during the events in Figure 7d. The refractory period is a period of time where no droplet detection events can occur and is represented by the gaps in the threshold detection in Figure 7e. The purpose of this period is to prevent

22

false positive detections if the injections are large and cause the droplet to expand backwards upstream and across the electrodes. For most situations, this timer is set to zero.
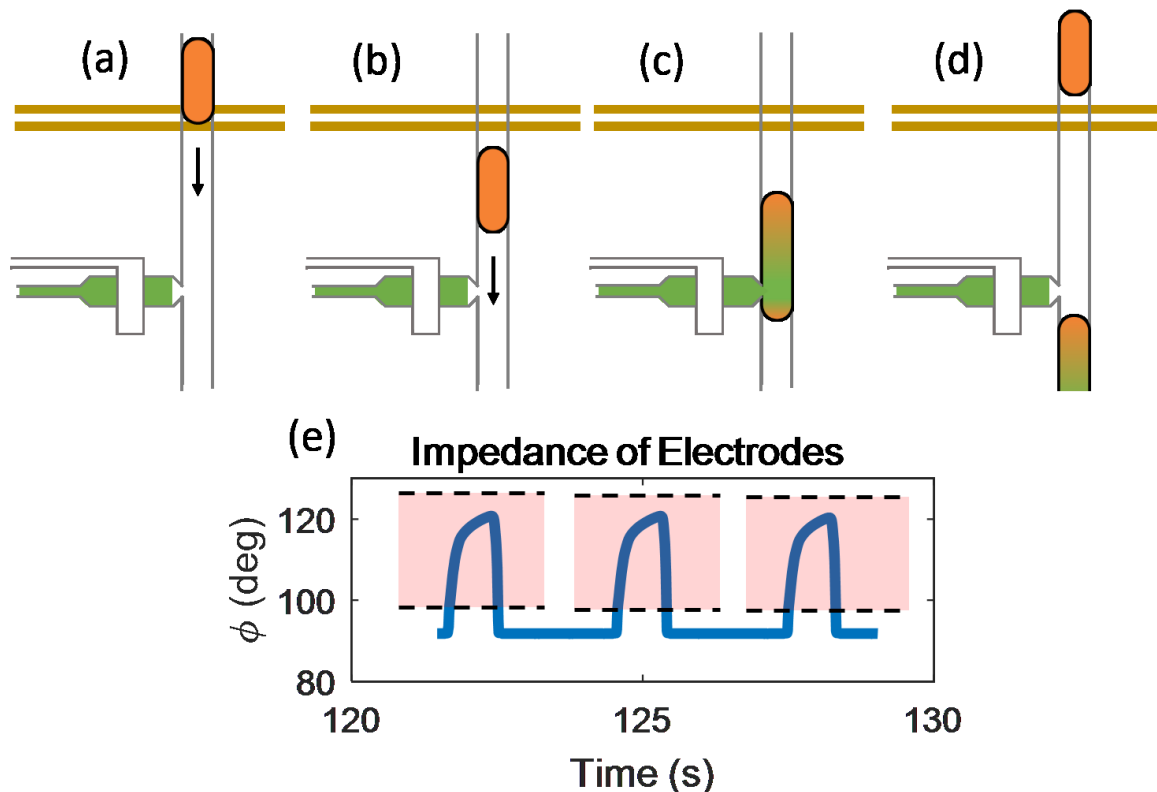

Figure 7: Schematic illustrating the stages of droplet detection and injection. (a) The detection event where the droplet initially reaches the electrodes. This correlates to a rise in the impedance phase as depicted in 5(e). (b) The droplet travel during the delay time period. (c) The open time period where the droplets are merged with reagent. (d) The refractory time period where the impedance measurements are ignored to prevent false positive detection. (e) A graph illustrating the impedance phase signal over time. The red regions represent the thresholds used to identify the presence of the droplet and the gaps represent the refractory period where the signals are ignored.

3   EXPERIMENTAL METHODS

During experimentation the prototype microfluidic device is filled with a silicone oil mixture (1:4 mixture of PFO in FC-40) for the continuous phase. The dispersed phase consists of a combination of DI water, food dye, and phosphate buffered saline

(PBS). The food dye is present to be able to visually identify the droplets in photographs of the device, while PBS was utilized to alter the impedance characteristics of droplets for content detection testing. In order to observe the system visually, the microdevice was mounted on an inverted microscope (IX71, Olympus), with a camera (70D, Canon™) affixed to the lens. Video tracking software (Tracker, Douglas Brown) was used to analyze the footage and track the instantaneous position and speed of droplets in the microdevice. Briefly, the tracking software works by selecting a subsection of pixels in any given frame and using it as an image template to define the position of a virtual point mass. The software then searches nearby in the following frames for a subset of pixels that most closely matches the RGB values of the original template and automatically marks the new point mass position. This position is relative to an axis and scale created on top of the first video frame, and the velocity of the point mass is derived from its position. For our image template, we selected the leading edge of any given droplet.

3.1 System Characterization

The preliminary set of experiments was aimed at characterizing this system and determining an optimal measurement frequency. Since impedance is a frequency-dependent property, and not all frequencies can be measured simultaneously, frequency choice is necessary to conduct real-time measurements. DI water droplets were generated at 0.5Hz frequency and transported through the microfluidic device before halting the flow so that a droplet was paused directly on top of the electrodes. Thereafter, commercial software included with the impedance

spectroscope (ziControl, Zurich Instruments) was utilized to sweep the frequency range from 10 kHz to 3 MHz. The flow was briefly restarted to expose the electrodes to only the continuous silicone oil and the frequency sweep was repeated. Afterwards, a few select frequencies were chosen to measure the impedance of traveling droplets in order to verify measurement consistency with operating conditions.

Since the primary goal of this system is to track droplet position for feedback control, a follow up experiment utilized an optimal measurement frequency to understand the dependence of the impedance signal on the droplet position above the electrodes. Low pressures are used to dramatically slow down the speed of the droplet to approximately 75 μm / second so the effects could be observed. The droplet position was recorded with the mounted camera and the impedance was simultaneously measured in order to understand how accurately droplet position can be measured.

3.2   Comparison to non-feedback systems

Following system characterization, a set of trials was designed to demonstrate the uncertainty in droplet position that exists in an open-loop control environment. The goal was to qualitatively determine the benefits of a feedback control system when compared to open-loop systems. For example, it has been shown in literature that the presence of droplets within a microfluidic device affects the resistance to fluid flow in pressure driven devices.[59] As our device is a pressure driven device, this implies that the speed of the droplets, and therefore their predicted positions, would

be affected by the amount of droplets in the device. An open-control system would need to account for these dynamics to accurately predict droplet position. In order to understand this effect, a new device was filled with the same silicone oil mixture as previous and droplets of DI water were generated at a rate of 0.2Hz. The speed of the droplets within the main fluid channel was measured after each droplet creation to determine the relationship between droplet count and droplet speed in this particular system. Also, during a droplet creation event, the transient behavior of droplets in the main fluid channel was recorded on video for analysis.

Finally, a direct comparison of the performance between the open-loop control and feedback control was made at steady state operating conditions. A microfluidic device is operating in steady state conditions when the frequency of droplets exiting the device is equal to the frequency with which they are created. This eliminates the uncertainties in droplet position stemming from the varying quantity of droplets in the device. When testing the open-loop control system, a periodic injection timer was created. The timing of this injection was initially set to match the programmed time between droplet creations, but from there it was finely tuned until at least 10 successful injections were made in sequence. After this point the following 100 droplets were observed and the number of successful injections recorded on video for review later. The trial was repeated for the system with feedback control to compare directly the injection success rate.

3.3 Content Detection and Combinatorial Demonstration

The final set of trials focused on investigating the capabilities of the impedance-based feedback system for droplet content detection and discretionary injection. For this, two samples were used to generate droplets in the droplet generation region of the microdevice. The first sample was comprised of DI water with green food dye while the second sample was a 10x concentration PBS mixed with red food dye in a 1:10 ratio. Droplets of these samples were generated at 0.2 Hz in a predetermined pattern and the impedance detection was utilized to identify and inject PBS droplets in various combinatorial patterns. Upon completion of the test, the flow was stopped in order for a panoramic photograph of the device to be captured.

4   RESULTS AND DISCUSSION

4.1   System Characterization

Frequency sweep data of the stationary droplets as compared to the peak values observed in traveling droplets are shown in Figure 8a. The optimal measurement frequency to separate the silicone oil mixture and DI water was found to be between 100 kHz and 200 kHz. It was observed that the peak measurements of the traveling droplets approximately followed the stationary sweeping data. It is therefore suggested that, with new fluids, the proper measurement frequency to distinguish the continuous phase from the dispersed phase can be found quickly with a stationary frequency sweep. In Figure 8b, a sample of the impedance signal at 200 kHz is shown while droplets travelled across the electrodes. It was noted that movement of the microscope stage or disturbances of the coaxial cables affected the magnitude

component of the impedance measurement, while the phase in contrast remained undisturbed. These disturbance scan be seen in Figure 8b in the upper chart. We therefore utilized phase measurement for threshold detection, as it was more reliable signal.

After frequency selection was performed, the system was tested for its positional accuracy. The largest change in impedance was found to correlate with the moment the front edge of the droplet bridged the gap between the electrodes as shown in Figure 9. The impedance signal continued to drastically change until the droplet completely covered the second electrode. In our device, the electrodes are designed to be 15 μm wide with a 10 μm gap in between. Therefore, if a threshold for droplet detection was set somewhere during the large impedance shift, the position of the front edge of the droplet would be on top of the second electrode, giving a positional accuracy equal to the width of the second electrode. However, it should be noted that the consistency would likely be much higher since this threshold-detected location would be nearly identical for the following droplet. The exact variance of positional determination of the droplet was not investigated in this paper, but the actual variation was likely to be less than half the width of the second electrode. It should also be noted that these results suggest that the hydrophobic coating utilized was not a perfect insulator, instead allowing current to directly pass through the droplets. If the hydrophobic coating was a perfect dielectric, then the signal would not change so suddenly upon bridging the gap between the electrodes but would be more gradual as the liquid permeated more of the potential electric field surrounding the electrodes.

(a) Static Drops vs Traveling Drops
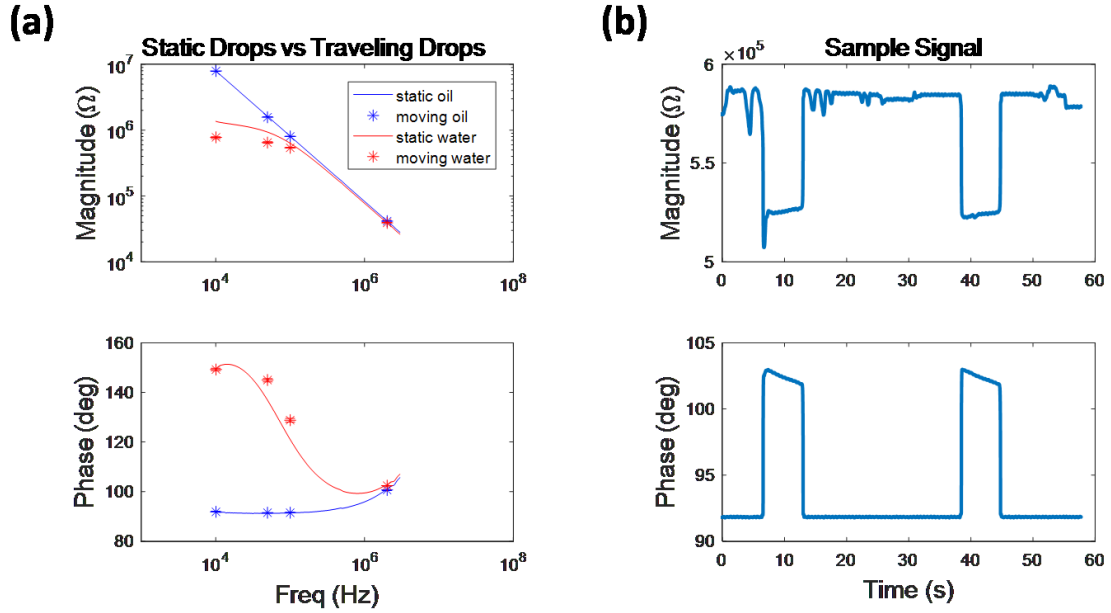
(b) Sample Signal

Figure 8: These charts illustrate the results of the system characterization trials. (a) The frequency sweep of stationary droplets vs the measurements of traveling droplets demonstrated that the traveling droplets have a trend that follows the frequency sweep but the measurements don't match exactly. (b) A sample of the impedance signal demonstrating the successful detection of DI water droplets suspended in the silicone oil mix.
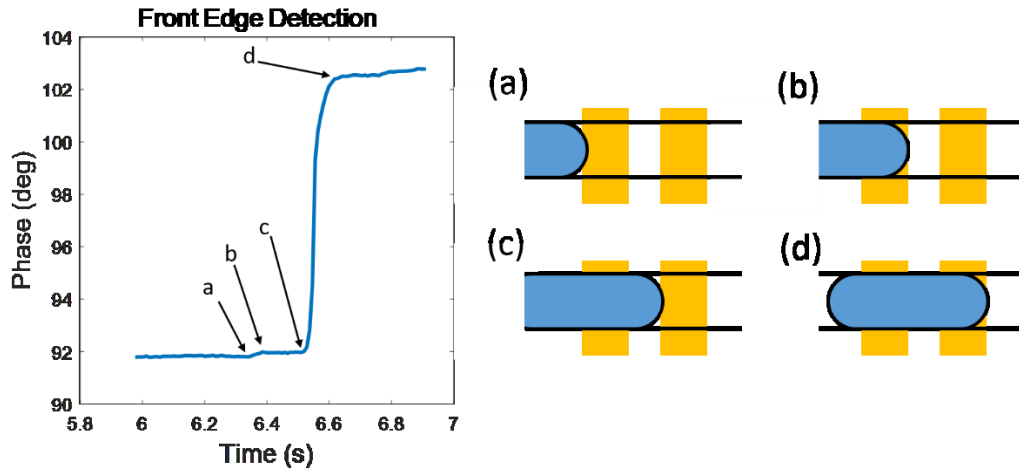

Front Edge Detection

Figure 9: An illustration of the impedance signal as based on droplet position. The chart shows real data collected while a DI water droplet passed over the electrodes and was measured at 200 kHz. The right illustrations show the droplet position that was observed at each feature of the impedance change. (a) When the front edge of the droplet first touched the first electrode, the phase began to shift linearly and stopped when (b) the droplet covered the entire electrode. However, the real impedance change occurred when (c) the droplet bridged the gap between the electrodes. This impedance change reached a stable point when the droplet covered both electrodes.

30

4.2   Droplet Velocity Uncertainty

In order for a device to have reliable open-loop control downstream injection the droplet position would have to be highly predictable. We measured the velocity of droplets through the device as a function of the number of droplets present and the resulting relationship between droplet velocity and droplet count is shown in Figure 10. Figure 10a reveals that the speed of the droplets is linearly dependent on the number of droplets in the device over a large range. Therefore, the exact number of droplets in the device should be known at all times in order to accurately predict droplet travel time over large distances. Additionally, it was observed that this speed change was not instantaneous and had some transience that would have to be accounted for as well. When the relief valves are opened during droplet generation, there is a temporary transience in the speed of the droplets throughout the device, as shown in Figure 10b. This change in speed is more dramatic with the droplets closest to the relief valves, but the effect is still noticeable for droplets farther away. Together, this data reveals the difficulties in predicting droplet position in microdevices with long droplet travel. Finally, it was also observed, but not reported on, that as droplets were injected, their larger size also affected the overall flow speed in the device.
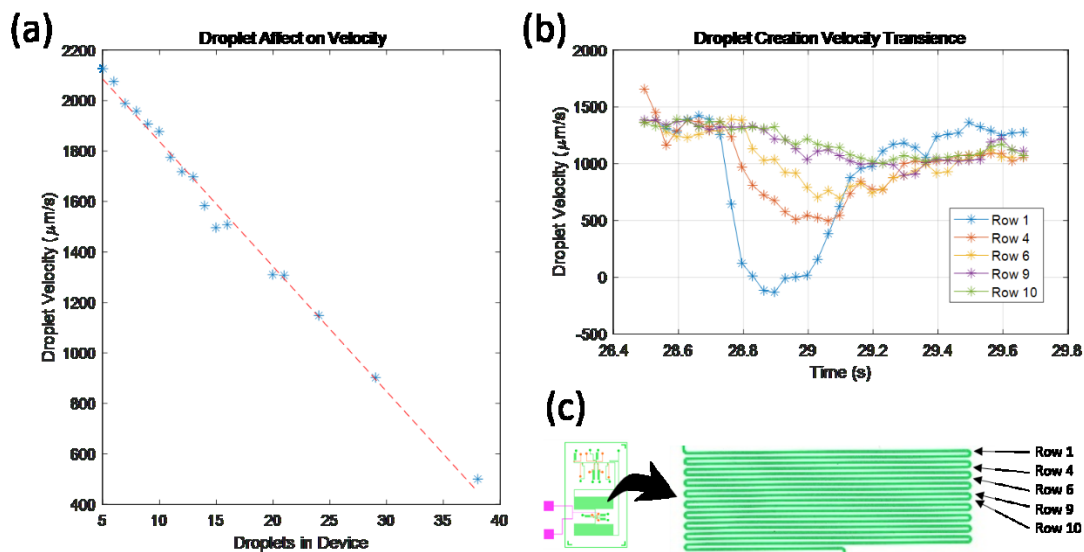
Figure 10: (a) The linear relationship between droplet count and droplet flow velocity in the chip is a strong fit. (b) This graph illustrates the droplet speed profile over the duration of a droplet creation event. Each line corresponds to a different position in the travel region. There is a clear transient behavior which is difficult to model and is dependent upon the droplet's position in the microdevice (c) This is a schematic illustrating the location of rows where the droplet velocity was measured in the device travel region. The droplets were generated above this region and the injection region was just below here.

4.3   Feedback vs Non-Feedback in an Optimized Setting

Although many droplet-quantity-dependent uncertainties exist as revealed above, these effects can be minimized if the number and size of droplets within the device is kept relatively constant. It was suspected, however, that even controlling for this wouldn't result in a successful open-loop control system due to numerous unknown compounding factors. We tested a microdevice operating in steady state and attempted to inject traveling droplets with an injection that was performed at regular time intervals. The results of this trial are summarized in Figure 11.

Figure 11a displays images of droplet injections since the start of the 100-serial attempts for both open-loop control and feedback control. After multiple

32

attempts at creating open-loop injection timers, the most optimal results obtained were 15 successful consecutive injections before the injections began to miss. An image of each corresponding droplet for the feedback system is shown next in parallel for visual comparison. After over 100 droplets, feedback system never missed an injection, as illustrated in Figure 11b. These results make clear that feedback control was necessary to have a successful injection in devices with a lot of travel time.
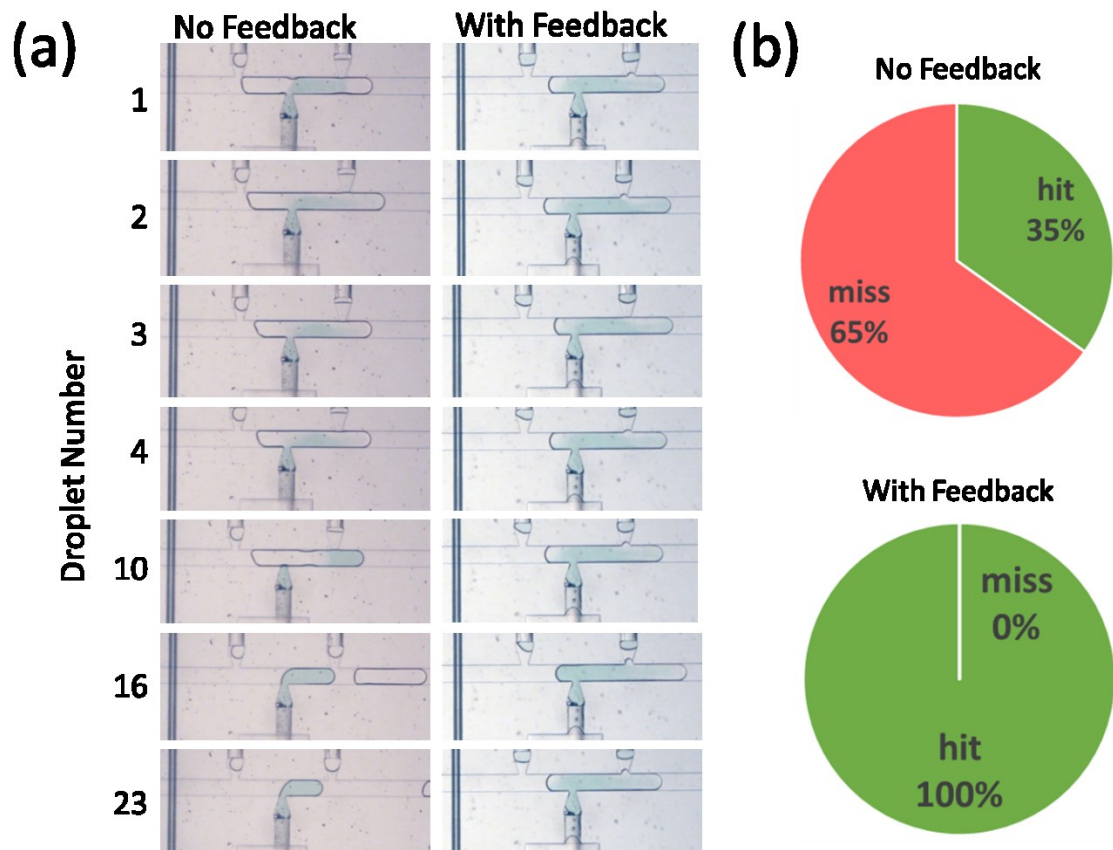
Figure 11: (a) A series of images demonstrating the reliability of the feedback system in contrast with the performance of the non-feedback system. The images were captured since each control system was initiated. The best result obtained for an open-loop control system was 15 successful injections before a 'miss' occurred. (b) The non-feedback and feedback systems were allowed to run for a series of 100 droplets. The pie charts represent the fraction of successful injection as compared to all attempted injections.

4.4   Content Detection and Discriminatory Injection

To explore the further capabilities of this system for droplet content detection, control droplets (green) and PBS droplets (red) were generated in a pattern of two PBS droplets in sequence followed by a single control droplet. 200 kHz was used as the measurement frequency and blue food dye was used as the injected reagent. A resulting sampling of the impedance signal demonstrates the difference observed between the control droplet and the PBS droplet and is shown in Figure 12a.

Threshold detection was employed to attempt to inject only the PBS droplets in the sequence with blue dye. After over 100 droplets injection attempts, 100% specificity and injection accuracy was observed. There were no green droplets that falsely received the blue injection, and there were no red droplets that missed an injection. The flow of oil was stopped and a panorama photograph of the device along with example before and after sequences is shown in Figure 12b. To additionally demonstrate the combinatorial capabilities of this technology, the microdevice was flushed with oil and the software was rewritten to only inject the first PBS droplet in each repetitive unit with blue dye. Figure 12c below highlights once again that the system had 100% specificity and 100% accuracy. There were no instances of the first PBS droplet not receiving blue dye, and no instances of control droplets of the second PBS droplets receiving blue dye as a false positive.
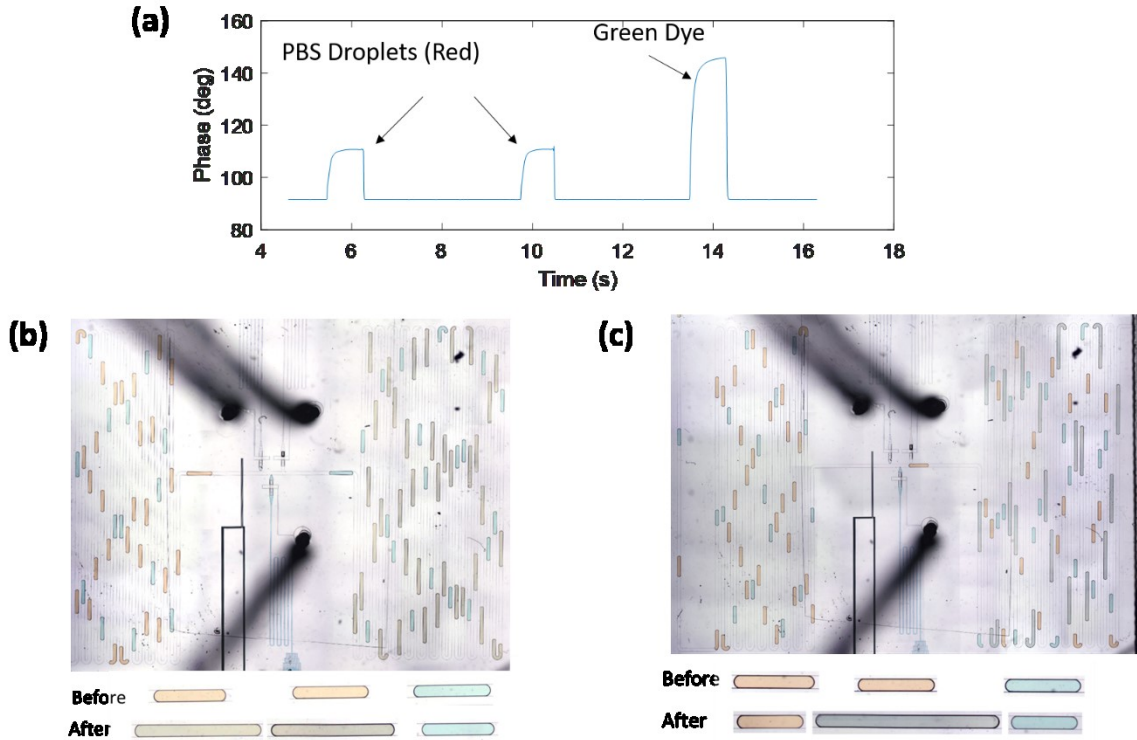
Figure 12: This figure illustrates the versatility of this feedback system to inject on demand content of the droplets as well as sequencing. In this experiment samples of red food dye were mixed with 10x PBS in a 1:10 ratio and compared to control droplets of green food dye. (a) A sample impedance signal from the electrode as the droplets pass over it. The difference in impedance is clear. (b) A panoramic image of the device when every PBS droplet was mixed with blue dye along with a sample series of droplets before and after the injection region. On the right side half of the photograph, a second travel region allows observation of the injection success. (c) A repeat attempt when the only the second PBS droplet was injected with blue dye, demonstrating the programmable capabilities of the system.

5   CONCLUSION

In this paper, we've presented a novel feedback control system for droplet-based microfluidic devices with microfluidic valves. The system utilized real-time impedance measurements of on-chip electrodes to control microfluidic valves for accurate downstream injections. The system was calibrated to track DI water droplets and PBS droplets suspended in silicone oil. Results indicated that the droplets were accurately identified and located as they traveled through the

microfluidic device. Furthermore, the uncertainty of droplet dynamics during long processing distances was demonstrated to justify the need for feedback control in downstream injection sites. Among the most important of these challenges was the resistance to flow as it was dependent on the number of droplets present within the device, but even in the absence of this factor it was shown to be near impossible to perform injections in an open-loop control system. The presented feedback system was shown to be effective in overcoming these challenges and effectively and reliably mixing droplets with the desired reagents. In addition, it was further presented that the functionality of this control system extends beyond basic positional detection to provide information about the droplet content as well. It was demonstrated that droplets could be discretionally mixed in a combinatorial manner dependent upon their electrical properties.

6 FUTURE DIRECTIONS AND PRELIMINARY RESULTS

6.1 Multiple Electrodes

Although this feedback control system shows great promise in future automation of microfluidic devices, the uncertainty in droplet speed could still present challenges in extreme conditions. For example, until steady state is reached, there is a large velocity difference between the first droplets that are generated and the final droplets that are generated. One possibility to eliminate this issue is to use a volumetrically driven system instead of a pressure driven device, but it is also possible to make this system more robust if the feedback measurements contained not only the droplet's position, but also its velocity. The current detection scheme could be simply expanded upon to derive the velocity of the droplet by adding another pair of electrodes. If the impedance of these pairs could be monitored independently, then the speed can be solved for by measuring the time difference between droplet detection events. In addition to speed, this system would also be able to characterize the length of the droplet. If the speed is known, then the width of the impedance signal would be indicative of the droplet length. The basic concept is illustrated in Figure 13. This would allow for accurate injections of systems that could even suffer from pressure or velocity variations.
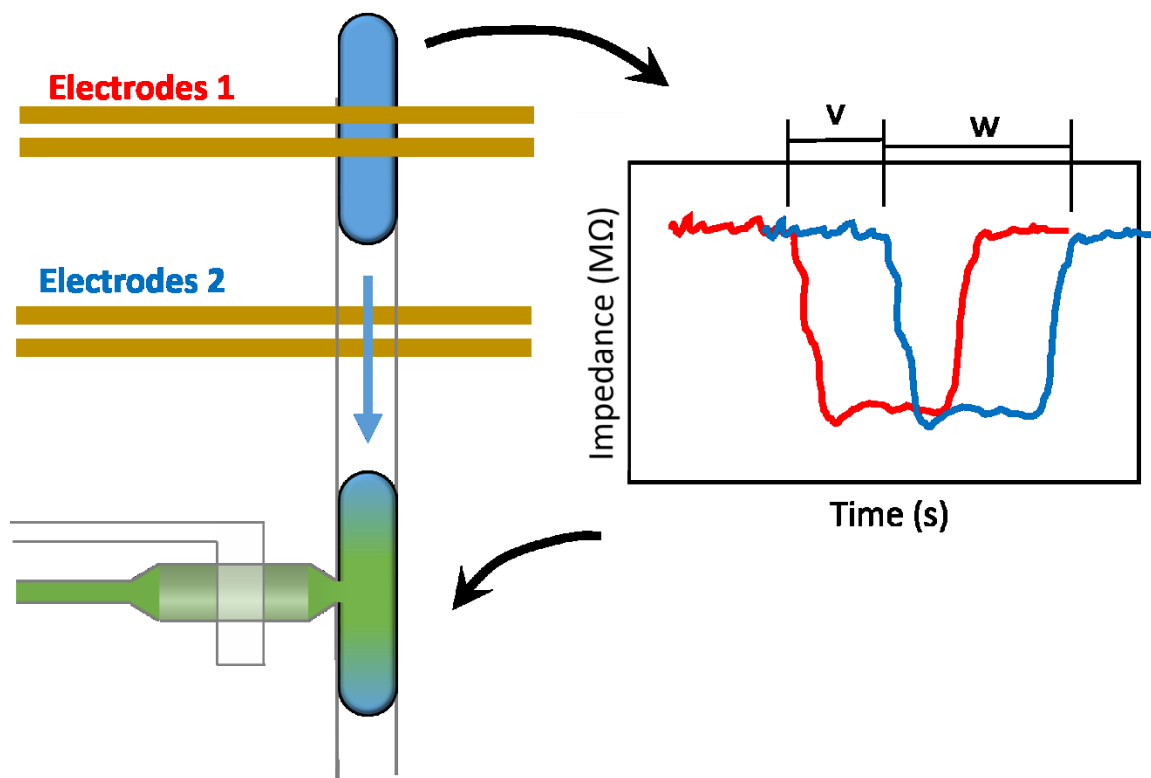
Figure 13: An illustration of the four electrode droplet detection system. The real time signal from each electrode is colored respectively and shown in the graph of real impedance. V represents the velocity of the droplet and is the difference between the droplet detection for each electrode. W is the width of the droplet and can be derived from the width of the signal.

6.2   PCR Precursor Potential

The system described in this paper could enable multistep multiplexing assays. One type of assay that could benefit from this system is any assay requiring a polymerase chain reaction (PCR) amplification step as a precursor to combinatorial screening. Instead of conducting amplification off of the device, this processing could occur all on a single microfluidic platform. One recent development of single nucleotide polymorphism (SNP) detection that could benefit from this technology is the Invader® assay. The Invader® assay is a highly specific and accurate system for detecting SNPs through fluorescence energy resonance transfer, but it sometimes

requires an initial PCR amplification step to obtain enough target molecules.[60] Detection of SNP in a continuous flow microfluidic device would be able to meet the needs of industrial applications that require high throughput genotyping systems such as disease detection or agricultural crop selection. It will need to be investigated, however, how the hydrophobic coating implemented in this study interacts with the PCR chemistry.

7 REFERENCES

1. Sutera, S. P. & Skalak, R. The History of Poiseuille Law. *Annu. Rev. Fluid Mech.* **25,** 1 (1993).
2. Terry, S. C., Herman, J. H. & Angell, J. B. A gas chromatographic air analyzer fabricated on a silicon wafer. *IEEE Trans. Electron Devices* **26,** 1880–1886 (1979).
3. Manz, A., Widmers, H. M. & Graber, N. Miniaturized total chemical analysis systems: A novel concept for chemical sensing. *Sensors Actuators B Chem.* **1,** 244–248 (1990).
4. Manz, A. *et al.* Planar chips technology for miniaturization and integration of separation techniques into monitoring systems. Capillary electrophoresis on a chip. *J. Chromatogr. A* **593,** 253–258 (1992).
5. Whitesides, G. M. The origins and the future of microfluidics. *Nature* **442,** 368–73 (2006).
6. Kikuchi, Y., Sato, K., Ohki, H. & Kaneko, T. Optically accesible microchannels formed in a single-crystal silicon substrate for studies of blood rheology. *Microvasc. Res.* **44,** 226–240 (1992).
7. Cokelet, G. R., Soave, R., Pugh, G. & Rathbun, L. Fabrication of in vitro microvascular blood flow systems by photolithography. *Microvasc. Res.* **46,** 394–400 (1993).
8. Shoji, S., Esashi, M. & Matsuo, T. Prototype miniature blood gas analyser fabricated on a silicon wafer. *Sensors and Actuators* **14,** 101–107 (1988).
9. Sutton, N., Tracey, M. C., Johnston, I. D., Greenaway, R. S. & Rampling, M. W. A novel instrument for studying the flow behaviour of erythrocytes through microchannels simulating human blood capillaries. *Microvasc. Res.* **53,** 272–81 (1997).
10. Burns, M. A. An Integrated Nanoliter DNA Analysis Device. *Science (80-.).* **282,** 484–487 (1998).
11. Effenhauser, C. S., Bruin, G. J. M., Paulus, A. & Ehrat, M. Integrated Capillary Electrophoresis on Flexible Silicone Microdevices: Analysis of DNA Restriction Fragments and Detection of Single DNA Molecules on Microchips. *Anal. Chem.* **69,** 3451–3457 (1997).
12. Duffy, D. & McDonald, J. Rapid prototyping of microfluidic systems in poly (dimethylsiloxane). *Anal. …* **70,** 4974–4984 (1998).
13. McDonald, J. C. *et al.* Fabrication of microfluidic systems in poly(dimethylsiloxane). *Electrophoresis* **21,** 27–40 (2000).
14. Regehr, K., Domenech, M. & Koepsel, J. Biological implications of polydimethylsiloxane-based microfluidic cell culture. *Lab Chip* **9,** 2132–2139 (2009).
15. Unger, M. A., Chou, H. P., Thorsen, T., Scherer, A. & Quake, S. R. Monolithic microfabricated valves and pumps by multilayer soft lithography. *Science* **288,** 113–6 (2000).
16. Thorsen, T., Roberts, R. W., Arnold, F. H. & Quake, S. R. Dynamic pattern

formation in a vesicle-generating microfluidic device. *Phys. Rev. Lett.* **86,** 4163–4166 (2001).

17.   Vyawahare, S., Griffiths, A. D. & Merten, C. A. Miniaturization and parallelization of biological and chemical assays in microfluidic devices. *Chem. Biol.* **17,** 1052–1065 (2010).

18.   Teh, S.-Y., Lin, R., Hung, L.-H. & Lee, A. P. Droplet microfluidics. *Lab Chip* **8,** 198–220 (2008).

19.   Dunn, D. A. & Feygin, I. Challenges and solutions to ultra-high-throughput screening assay miniaturization: Submicroliter fluid handling. *Drug Discov. Today* **5,** S84–S91 (2000).

20.   Yin, H. *et al.* Quantitative comparison between microfluidic and microtiter plate formats for cell-based assays. *Anal. Chem.* **80,** 179–185 (2008).

21.   Warrick, J., Meyvantsson, I., Ju, J. & Beebe, D. J. High-throughput microfluidics: improved sample treatment and washing over standard wells. *Lab Chip* **7,** 316–321 (2007).

22.   Weinmeister, R., Freeman, E., Eperon, I. C., Stuart, A. M. & Hudson, A. J. Single-Fluorophore Detection in Femtoliter Droplets Generated by Flow Focusing. *ACS Nano* **9,** 9718–9730 (2015).

23.   Mazutis, L. *et al.* Single-cell analysis and sorting using droplet-based microfluidics. *Nat. Protoc.* **8,** 870–891 (2013).

24.   Juul, S. *et al.* A Droplet Microfluidics Platform for Highly Sensitive and Quantitative Detection of Malaria Causing Plasmodium Parasites Based on Enzyme Activity Measurement. **6,** 10676–10683 (2013).

25.   Hess, D., Rane, A., Demello, A. J. & Stavrakis, S. High-throughput, quantitative enzyme kinetic analysis in microdroplets using stroboscopic epifluorescence imaging. *Anal. Chem.* **87,** 4965–4972 (2015).

26.   Xu, J. H., Li, S. W., Tán, J., Wang, Y. J. & Luo, G. S. Preparation of highly monodisperse droplet in a T-junction microfluidic device. *AIChE J.* **52,** 3005–3010 (2006).

27.   Umbanhowar, P. B., Prasad, V. & Weitz, D. A. Monodisperse emulsuion generation via drop break-off in a co-flowing stream. *Langmuir* 1–22 (1999).

28.   Anna, S. L., Bontoux, N. & Stone, H. A. Formation of dispersions using 'flow focusing' in microchannels. *Appl. Phys. Lett.* **82,** 364–366 (2003).

29.   Zhu, P. & Wang, L. Passive and active droplet generation with microfluidics: a review. *Lab Chip* **17,** 34–75 (2017).

30.   He, M., Kuo, J. S. & Chiu, D. T. Electro-generation of single femtoliter- and picoliter-volume aqueous droplets in microfluidic systems. *Appl. Phys. Lett.* **87,** 14–17 (2005).

31.   He, M., Kuo, J. S. & Chiu, D. T. Effects of ultrasmall orifices on the electrogeneration of femtoliter-volume aqueous droplets. *Langmuir* **22,** 6408–6413 (2006).

32.   Park, S.-Y., Wu, T.-H., Chen, Y., Teitell, M. A. & Chiou, P.-Y. High-speed droplet generation on demand driven by pulse laser-induced cavitation. *Lab Chip* **11,** 1010 (2011).

33.   Xu, J. & Attinger, D. Drop on demand in a microfluidic chip. *J. Micromechanics Microengineering* **18,** 65020 (2008).

34. Churski, K., Korczyk, P. & Garstecki, P. High-throughput automated droplet microfluidic system for screening of reaction conditions. *Lab Chip* **10,** 816–818 (2010).

35. Bo-Chih, L. & Yu-Chuan, S. On-demand liquid-in-liquid droplet metering and fusion utilizing pneumatically actuated membrane valves. *J. Micromechanics Microengineering* **18,** 115005 (2008).

36. Zeng, S., Li, B., Su, X., Qin, J. & Lin, B. Microvalve-actuated precise control of individual droplets in microfluidic devices. *Lab Chip* **9,** 1340 (2009).

37. Song, H., Tice, J. D. & Ismagilov, R. F. A microfluidic system for controlling reaction networks in time. *Angew. Chemie - Int. Ed.* **42,** 768–772 (2003).

38. Tan, Y.-C., Fisher, J. S., Lee, A. I., Cristini, V. & Lee, A. P. Design of microfluidic channel geometries for the control of droplet volume, chemical concentration, and sorting. *Lab Chip* **4,** 292–298 (2004).

39. Niu, X., Gulati, S., Edel, J. B. & deMello, A. J. Pillar-induced droplet merging in microfluidic circuits. *Lab Chip* **8,** 1837–1841 (2008).

40. Link, D. R. *et al.* Electric control of droplets in microfluidic devices. *Angew. Chemie - Int. Ed.* **45,** 2556–2560 (2006).

41. Zagnoni, M. & Cooper, J. M. On-chip electrocoalescence of microdroplets as a function of voltage, frequency and droplet size. *Lab Chip* **9,** 2652–8 (2009).

42. Sesen, M., Alan, T. & Neild, A. Microfluidic on-demand droplet merging using surface acoustic waves. *Lab Chip* **14,** 3325 (2014).

43. Yoon, D. H. *et al.* Active microdroplet merging by hydrodynamic flow control using a pneumatic actuator-assisted pillar structure. *Lab Chip* **14,** 3050–5 (2014).

44. Varma, V. B., Ray, A., Wang, Z. M., Wang, Z. P. & Ramanujan, R. V. Droplet Merging on a Lab-on-a-Chip Platform by Uniform Magnetic Fields. *Sci. Rep.* **6,** 37671 (2016).

45. Gerdts, C. J. *et al.* Time-controlled microfluidic seeding in nL-volume droplets to separate nucleation and growth stages of protein crystallization. *Angew. Chemie - Int. Ed.* **45,** 8156–8160 (2006).

46. Song, H., Li, H. W., Munson, M. S., Ha, T. G. Van & Ismagilov, R. F. On-chip titration of an anticoagulant argatroban and determination of the clotting time within whole blood or plasma using a plug-based microfluidic system. *Anal. Chem.* **78,** 4839–4849 (2006).

47. Shestopalov, I., Tice, J. D. & Ismagilov, R. F. Multi-step synthesis of nanoparticles performed on millisecond time scale in a microfluidic droplet-based system. *Lab Chip* **4,** 316–321 (2004).

48. Abate, A. R., Hung, T., Mary, P., Agresti, J. J. & Weitz, D. a. High-throughput injection with microfluidics using picoinjectors. *Proc. Natl. Acad. Sci. U. S. A.* **107,** 19163–19166 (2010).

49. Tangen, U., Sharma, A., Wagler, P. & McCaskill, J. S. On demand nanoliter-scale microfluidic droplet generation, injection, and mixing using a passive microfluidic device. *Biomicrofluidics* **9,** 1–17 (2015).

50. Rane, T. D., Zec, H. C. & Wang, T. A Barcode-Free Combinatorial Screening Platform for Matrix Metalloproteinase Screening. *Anal. Chem.* **87,** 1950–1956 (2015).

51. Armani, M., Chaudhary, S., Probst, R., Walker, S. & Shapiro, B. Control of microfluidic systems: Two examples, results, and challenges. *Int. J. Robust Nonlinear Control* **15,** 785–803 (2005).
52. Schwartz, J. A., Vykoukal, J. V & Gascoyne, P. R. C. Droplet-based chemistry on a programmable micro-chip. *Lab Chip* **4,** 11–17 (2004).
53. Srivastava, N. & Burns, M. a. Electronic drop sensing in microfluidic devices: automated operation of a nanoliter viscometer. *Lab Chip* **6,** 744–51 (2006).
54. Kubra Isgor, P., Marcali, M., Keser, M. & Elbuken, C. Microfluidic droplet content detection using integrated capacitive sensors. *Sensors Actuators, B Chem.* **210,** 669–675 (2015).
55. Ren, H., Fair, R. B. & Pollack, M. G. Automated on-chip droplet dispensing with volume control by electro-wetting actuation and capacitance metering. *Sensors Actuators, B Chem.* **98,** 319–327 (2004).
56. Sadeghi, S. *et al.* On chip droplet characterization: A practical, high-sensitivity measurement of droplet impedance in digital microfluidics. *Anal. Chem.* **84,** 1915–1923 (2012).
57. Thomson, M. J. High-Throughput SNP Genotyping to Accelerate Crop Improvement. *Plant Breed. Biotechnol.* **2,** 195–212 (2014).
58. Rafael Gómez-Sjöberg. USB-Based Controller. *Google Sites* Available at: https://sites.google.com/site/rafaelsmicrofluidicspage/valve-controllers/usb-based-controller. (Accessed: 17th April 2017)
59. Baroud, C. N., Gallaire, F. & Dangla, R. Dynamics of microfluidic droplets. *Lab Chip* **10,** 2032 (2010).
60. Olivier, M. The Invader?? assay for SNP genotyping. *Mutat. Res. - Fundam. Mol. Mech. Mutagen.* **573,** 103–110 (2005).

8 CURRICULUM VITAE

Brant Axt

612-750-5330

brantaxt@gmail.com

EDUCATION

Masters of Science in Biomedical Engineering (expected May 2017)

Johns Hopkins University, Baltimore, MD

Bachelors of Science in Mechanical Engineering (May 2015)

University of Minnesota-Twin Cities, Minneapolis, MN

Summa Cum Laude

Dean's List all semesters

PROFRESSIONAL EXPERIENCE

Research Assistant, Johns Hopkins University   Sep 2015 – Present

Baltimore, MD

- Independently conduct microfluidic device research on integrated impedance sensing
- File a provisional and non-provisional utility patent
- Teaching Assistant and Grader to undergraduate courses in engineering
- Published conference poster on impedance feedback control in microfluidics
- Use MATLAB to develop user interface for modifying feedback program
- Use photolithography to fabricate microfluidic devices weekly

Technical Intern, Medtronic   May 2015 – Sep 2015

Brooklyn Center, MN

- Studied lean manufacturing and applied it to redesign u-cells on manufacturing floor
- Developed a new system to track employee training and decrease down time
- Collaborated with engineers in molding and continuous improvement

Research Assistant, University of Minnesota   Feb 2014 - May 2015

Minneapolis, MN

- Investigate tissue moisture content measurement using impedance
- Coauthored conference paper in Design of Medical Devices Conference

Technical Intern, Medtronic   May 2014 – May 2015

Mounds View, MN

- Create and manage logistics for long term material additive study
- Performing insertion force testing for new lead connection standards
- Use MINITAB to analyze statistically significant results
- Use LabVIEW to design tool interface programs for legacy equipment

Technical Intern, Medtronic   May 2013- May 2014

Brooklyn Center, MN

- Use Pro/ENGINEER to design tooling for improved ergonomics
- Use JavaScript, HTML5, and JSON to design and implement equipment database prototype

PUBLICATIONS

"Wearable Coplanar Capacitive Sensor for Measurement of Water Content – A Preliminary Endeavor" presented at the Design of Medical Devices Conference, Minneapolis 2016

"Fully Automated Operation of Microfluidic Device with Impedance Based Valve Control" presented at the conference for Miniaturized Systems for Chemistry and Life Sciences, Dublin, 2016